

UCRL-2161
Unclassified-Physics Distribution

UNIVERSITY OF CALIFORNIA

Radiation Laboratory

Contract No. W-7405-eng-48

35330

**EMPLOYMENT OF THE SPIRAL ORBIT SPECTROMETER
TO MEASURE PION PRODUCTION RATIOS BY PROTON BOMBARDMENT**

Ryokichi Sagane

May 26, 1953

Berkeley, California

**EMPLOYMENT OF THE SPIRAL ORBIT SPECTROMETER
TO MEASURE PION PRODUCTION RATIOS BY PROTON BOMBARDMENT**

Ryokichi Sagane

Radiation Laboratory, Department of Physics,
University of California, Berkeley, California

May 26, 1953

ABSTRACT

Plus-minus ratios for pion production by 340-Mev proton bombardment were measured at 13 Mev, 18 Mev, and 42 Mev with the use of the spiral orbit spectrometer.

Mesons of known energy intervals emitted at 90° produced by the proton beam at the target on the axis were efficiently detected by the C2, 200 μ plates located near the outer edge of the pole pieces.

Out of the results obtained by scanning the plates, the π^+/π^- ratios at three energies from Be, C, Al, Cu, Ag, and Pb targets were obtained. A rough estimate of the Z dependence of π^+ production at 42 Mev was also made.

Since the spiral orbit spectrometer was found to be quite useful for this kind of experiment, experimental details and some of the results of the tests are given.

**EMPLOYMENT OF THE SPIRAL ORBIT SPECTROMETER
TO MEASURE PION PRODUCTION RATIOS BY PROTON BOMBARDMENT**

Ryokichi Sagane

**Radiation Laboratory, Department of Physics,
University of California, Berkeley, California**

May 26, 1953

INTRODUCTION

In the study of the production of charged π -mesons in nucleon-nucleus collisions, the π^+/π^- ratio is a quantity suitable for the comparison of experimental results and the theoretical calculations.

Generally speaking, the mechanism of the meson production due to nucleon-nucleus collision is too complicated to be compared with theories and to gather information about the choice of assumptions or approximations in different theories. Yet it has been pointed out that not only the basic production processes in nucleon-nucleus collisions, but also some more detailed effects should be taken into account. For example, the effect due to the finite nucleon momenta inside of nuclei, the effect due to the Coulomb field, and the effect due to the nucleon collisions with the produced mesons before emission are among the factors to be taken into consideration. As far as these effects are concerned, some developments of theories have been made and are about ready to compare with experiments.

From the experimental point of view, π^+/π^- ratios have been measured since shortly after the discovery of the artificial mesons. Most of these earlier experiments were made inside the cyclotron vacuum chamber with the use of separate channels and different plates for π^+ and π^- mesons. Since these two points have introduced some ambiguities and inaccuracies, the later experiments were made mostly with the use of the same detector plates for both π^+ and π^- mesons.

Two kinds of techniques have been used on this line. The first one was developed by Drs. C. Richman and H. A. Wilcox³ using the external proton beam. Mesons produced at the target and emitted at 90° from the target were detected by nuclear plates embedded in a set of copper wedge absorbers. The

second one was developed by Dr. W. Barkas et al.³ using the internal beam of the cyclotron. The detector plates were put several inches below the plane of the circulating beam, embedded in a set of copper wedge absorbers. Both positive and negative mesons emitted downward from the target were thus detected. Since the lines of force of the magnetic field of the cyclotron are parallel to the motion of the mesons, the influence of the magnetic field is small and, consequently, the difference of the effects for the π^+ and π^- is nearly negligible. The proton beam intensity was monitored by the use of the induced radioactivity produced in the thin polystyrene foils placed in front of the targets. Almost the same technique was adopted by the Columbia University group, Block et al.³, later.

The data obtained so far gave mostly some rough ideas of the meson spectra and the π^+/π^- ratios, but in most of the cases, the accuracies were not always satisfactory, mainly because of the poor statistics. In general, the exposed plates in the two kinds of techniques suffered from high background and this not only made the scanning harder but also limited the exposure time of the bombardment.

Since the spiral orbit spectrometer provides almost 2π angular focusing, and has other features which make it well adapted for the measurement of the π^+/π^- ratios, the author has carried out a number of measurements to improve the accuracies of some of the results on the π^+/π^- ratios.

The present experiments cover only three energies and data are lacking at high energies to compute π^+/π^- ratios for the total cross sections. An experiment on the Z-dependence of π^+ and π^- production as a function of energies is now being carried out, however. From the data on Z-dependence, one can automatically calculate the π^+/π^- ratios at each energy so that one can expect that more accurate information on the integral ratios will be provided.

EXPERIMENTAL CONDITIONS

The 340 Mev protons deflected out from the cyclotron were collimated to either 1 inch or 1/2 inch O. D. and were passed through a 1-1/2 inch I. D. hole on the axis of the 20-inch O. D. pole pieces of a large electromagnet. Focusing of 8 Mev pions was obtained with a 2-5/8 inch gap, and of 13 Mev pions with a 1-1/8 inch gap. Energy loss through the target material was more significant for the energy spread than the resolution of the spectrometer. As

a result, these settings corresponded to average energies of 13 Mev and 18 Mev, respectively. Use of a tubular absorber (10 mm wall, Cu) at the 8 Mev setting made possible the detection of 42 Mev mesons.

Two 1-inch x 3-inch Ilford C2, 200 μ plates were put together with emulsion side face to face, so that a thickness of 400 μ of emulsion covered by 1 mm thick glass absorbers on each side was available for pion detection of both signs. Since the range of 8 Mev pions is about 1.5 mm in emulsion, one or two layers of 5 mil copper foils were added so that the number of pion endings would be equally shared by the plates. As shown in Fig. 1, mesons of right momentum approach the stable orbit, following the illustrated type of a spiral trajectory, and hit the plates mounted behind the radiation shield with surfaces perpendicular to the incoming mesons.

Because of the fact that the detectors were located about 11 inches from the target at 90° relative to the proton beam and shielded against radiation from the target by a 2-inch lead brick and a stack of wolfram plates of about 1-inch thick, the background proton tracks caused by neutrons were quite small in number. As a result, it was possible to make ample exposures so that the density of mesons in the plates was quite high and still keeping the background reasonably low. Scanning of about 50-200 pions per eight hours was easily made for the plates properly exposed.

Scanning was made over the same central area on the plates with a criterion not to count the events which occurred within 10 microns from the top and bottom surfaces of the emulsion. The number of π - μ decay was taken as the number of π^+ endings. The number of π^- stars with one or more prongs (π^- stars with one club were not taken as one prong stars) were counted. The number of π^- endings was derived by dividing this number by a factor 0.69, which is the known (and also checked) probability of having one or more prongs in π^- stars (as shown in Fig. 8 and discussed later).

Determination of detection efficiencies for π^+ - μ^+ decay and π^- stars was made by scanning the same plates several times. The results were not always the same, but 90 percent for π - μ decays and 97 percent for π^- stars seems to be adequate for evaluation of π^+/π^- ratios.

The main features of the present technique adopted here are as follows:

(1) Conditions for absorption through the target and for focusing close to the stable orbit are symmetric for both signs of pions.

(2) Both energy resolution and angular acceptances are the same for both signs. (Both the masses and the life times for π^+ and π^- are assumed to be exactly the same.)

(3) Since the same emulsion is used for detection of both signs of pions, the results obtained are entirely free from ambiguities due to the differences in emulsion thickness and developments, although the detection efficiencies for π^+ endings and π^- stars are not the same.

(4) π^+/π^- ratios can be obtained based on the numbers of π^+ and π^- detected on the same run, on the same target and with the use of the same absorber.

(5) Very low proton background tracks.

Accordingly, the spiral orbit spectrometer is deemed to be quite suited for the study of π^+/π^- ratios. Of course, it is also suited for meson production studies. But, due to the effect of scattering through the absorbers and the target itself, calibrations for solid angles corresponding to each energy setting are always required for this purpose.

RESULTS

The results of the scanning and the dimensions of the targets used were tabulated in Table I and Table II.

1. π^+/π^- Ratios.

The Table III gives the summary of the π^+/π^- ratio at three different energies on Pb, Ag (Sn), Cu, Al, C, and Be. This shows the following tendencies:

(a) The effect of Coulomb field of nuclei reduces the number of π^+ at low energies. As a result, π^+/π^- ratios are all relatively low for 13 Mev. At even 18 Mev this effect is evident for heavy elements such as Pb, Ag, and Cu.

(b) For each of the elements the ratios were highest at 42 Mev and lowest at 13 Mev.

(c) For each of the energies the ratios are high for Al and C and relatively low for Pb, Ag, and also for Be.

Due to the effectiveness of the spiral orbit spectrometer, these results were obtained with better statistical accuracies than most of the results so far reported. Furthermore, because of the very low intensity of background proton tracks, as mentioned above, the probability of the accidental coincidence of a

proton track beginning at the end of a μ meson track was negligible. Actually, the number of meson tracks and the number of background proton tracks were in most cases around one to one or, in the worst case, one to five in ratio.

The results obtained here for π^+/π^- ratios are in general in rough agreement with most of the results so far reported.³ But there are several cases which disagree by a factor of two or three. An effort has been made to look for causes of these discrepancies, but no effect of sufficient importance has been found except the statistical errors. The author expects to gather the same type of information in the course of the experiment on Z-dependence which is now under way. He expects that this will give more definite information.

The choice of the shapes and the dimensions of the targets was made so as to have the same order of energy loss for the incident protons in each target and also to have approximately the same absorption for outgoing mesons. As a result, cylindrical or tubular shapes were adopted for light elements and a conical shape of proper thickness was adopted for heavy elements as shown in Table I and II. The energy resolutions of the present experiment were calculated as the sum of the resolution of the spectrometer and the energy spread caused by the absorption through the targets. The half widths of the energy spread corresponding to each energy are given in the tables.

2. Z-Dependence of π^+ Production of 42 Mev.

Although the monitoring of the proton beam intensity was not properly made, the relative number of protons for each exposure made on the same day can be roughly estimated from the exposure time, since the proton beam intensity stayed almost constant within 10-15 percent of accuracy during an hour or two of running on the same day. Relative cross sections of π^+ production at 42 Mev were calculated from the results of scanning and plotted versus the atomic number of the target material. As shown in Fig. 2, the plot shows a clear $Z^{2/3}$ dependence rather than Z^1 dependence for high Z elements and a little ambiguous for low Z elements. Further experiments on this problem are now going on as mentioned above.

FURTHER EXPERIMENTAL DETAILS

1. Focusing Obtained by the Spiral Orbit Spectrometer.

The magnetic field intensity distributions on the median plane versus distance from the axis on the 2-5/8 inch gap and 1-1/8 inch gap are given in Fig. 3 and Fig. 4 respectively. Corresponding to each distribution, $\int H r dr$ and $H r^2$

were plotted as shown in the figures. The intersection of these plots gives the value of p which satisfies the condition for the stable orbit of the spiral orbit spectrometer.¹

$$\int_0^p Hr dr = Hp^2$$

As has been well known, the position of p , the position of the "stable orbit", corresponds to the position of $1/r \int Hr dr = \max$, or \bar{A}_{\max} (the vector potential). The radius of curvature at the point p of the plot of the vector potential \bar{A} versus radius is rather important in the theory of the spiral orbit spectrometer.

A parameter χ , defined by the formula $\chi^2 = 2/n-1$ where $n = -r/H$ dH/dr , has been introduced in the theory. The parameter χ is proportional to the radius of curvature of the plot of the vector potential versus radius at $r = p$.

Depending on the field distribution close to the stable orbit, the rate of approach to the stable orbit by the trajectory of a charged particle emitted on the axis is different. If $\chi > 1$, the trajectory approaches the stable orbit gradually. If $\chi < 1$, the approach is much more rapid.

It has not been thoroughly studied as yet what value of χ may give the best compromise between resolution in momentum and adequate density on the plates.

In Fig. 5 is shown a plot of the number of mesons found in the emulsion as a function of distance from the axis. (The value of χ for this case was $\chi = 1.5$, corresponding to the case of the 2-5/8 inch gap.) This plot gives a rough idea of the focusing of charged particles with the use of the spiral orbit spectrometer.

Since the magnetic field intensity is decreasing for increasing r , the distance from the axis, a vertical focusing is also expected. According to the theory of the spiral orbit spectrometer, the Z-component of the trajectory makes an up and down oscillation relative to the median plane in the course of approaching the stable orbit. The formula for this oscillation has been given as¹

$$Z \sim C_1 \sin \left(a_1 \sqrt{1 + \frac{2}{\chi^2}} \cdot t \right) \quad t = \text{time}$$

$$\sim C_2 \sin \left(a_2 \sqrt{1 + \frac{2}{\chi^2}} \cdot \theta \right) \quad \theta = \text{angle of revolution}$$

This means that charged particles emitted a little off in direction from 90° or charged particles emitted somewhat off in position from the median plane are expected to oscillate up and down relative to the median plane as they approach close to the stable orbit.

If $X \ll 1$ as in the 1-1/8 inch gap, the period of this vertical oscillation is much shorter than the period of angular revolution, while if $X > 1$ or $X = 1.5$ as in the 2-5/8 inch gap, the period of this vertical oscillation is comparable to or longer than the period of revolution. As a result, use of $X > 1$ should yield a high density of charged particles close to the median plane, while the case $X < 1$ should give almost uniform intensity across the gap because most of the mesons will oscillate up and down several times before they reach to the detector.

The plots given in Fig. 6 represent the number of mesons found in the plates as a function of X . These two plots support nicely the prediction derived from the theory of the spiral orbit spectrometer.

This focusing effect is rather important because one can gain by at least a factor 3-10 by focusing particles emitted within an interval of several degrees from 90° , and also focusing particles emitted in an interval of several centimeters from the median plane. The latter indicates the advantage of using a reasonably wide gap with a target traversing the whole gap for neutron runs and also for x-ray runs. Because of the focusing, the mesons created apart from the median plane may still be collected close to the median plane.

2. Computation of a Gain in Intensity in the Present Experiment.

The intensity distribution versus the distance from the median plane, as shown in Fig. 6, gives a rough idea of the gain in intensity due to the vertical focusing compared with the case with no focusing. A factor of three is obtained if (a) the scanning is done ± 7 mm only, relative to the median plane, and (b) the intensity without the vertical focusing is assumed to be the mean value of the total integral of the plot.

As for the horizontal focusing, nearly 315 degree focusing was accomplished, which means a factor of 20-60 compared with the usual 15° - 5° coverage. But the momentum resolution of the spectrometer was roughly ± 3 percent, which was better than necessary compared with the energy spread caused by some other reasons. This reduces the intensity by a factor 3-10 (especially for the high energy settings using absorbers). It has been found that a special type of magnetic field distribution may give a larger ΔH_p , so that one can reduce this factor almost to

unity. By taking into account the effect due to the life time of pions discussed later, the overall improvement in intensity or density of mesons gained by the present technique is about 3-30 compared with the case of mere deflection.

Furthermore, the area of emulsion of having the above density is usually of the order of 15 mm x 20 mm or more, which is larger by a factor 3-20 compared with the use of a 15° wedge absorber in the deflection method.

As a result, the present technique seems to reduce by a factor of 10-600 the exposure time required in order to get the same number of pions at the detector.

3. Effect of the Life Time.

Since the mean life for π -mesons has been measured as 2.55×10^{-8} sec, some of the pions were lost due to their decay in flight. For this reason, it is desirable to use higher magnetic field and to reduce the distance from the source to the detector. The loss due to the life time amounted in the present experiment to from 15 percent up to 45 percent, depending on the azimuthal angle of emission from the target relative to the position of the plates. As can be seen clearly in Fig. 1, lengths of path for pions vary from 15 inches up to 60 inches.

4. Detection of Mesons with Perpendicular Incidence into the Plates.

It is to be mentioned that the conditions are quite different for detection of almost monoenergetic and nearly parallel mesons compared with the case of usual poor geometry experiments. The reasons why the usual tilted (15° - 20°) position of plates relative to the direction of incoming meson flux was not adopted here are as follows:

(a) The density of mesons to be found in the emulsion is proportional to $\sin \theta$ and $\theta = 90^\circ$ gives maximum density.

(b) Due to the scattering at the absorber in front of the emulsion, incident angles for mesons into the emulsion are mostly quite different from 90° .

The probability of making not only small angle scatterings but making large angle scatterings is also appreciable, especially toward the end of the range. As a result, one can expect fairly long average path lengths of pions inside of the emulsion before they stop. On the other hand, due to the low background, not much ambiguity exists for most of the meson tracks so that the required minimum path length to identify tracks as those of pions is relatively shorter than in the case with high background.

5

Yet, one should admit that the probability of having very short pion tracks associated with very short muon tracks or nucleon tracks is certainly high compared with the case for tilted plates. This may cause a low detection efficiency but this loss is only a few percent.

The author is of the opinion that the gain of a factor of about 3 (arising from the larger value of $\sin \theta$), which increased the number of events and decreased the statistical error, compensated the decrease in detection efficiency.

(c) The thickness of glass plates of C2 plates was about 1 mm. The most efficient use of the magnet was obtained at 8 Mev setting. The range of 8 Mev pions is about 1.5 mm in emulsion. This fact was the main reason for selecting $\theta = 90^\circ$.

5. The Projected Range Straggling Curve for 8 Mev Pions.

It has been well known that mesons suffer mostly small angle scattering during their passage through the absorber, and when they approach close to the end of their ranges they also suffer from large angle scattering.

Since mesons were detected by identifying their endings only, some rough idea about the projected range straggling curve is needed in order to calculate the absolute detection efficiency for the incoming meson flux.

This was done by adjusting the slit system of the spiral orbit spectrometer so that the energy resolution was ± 2 percent for 8 Mev mesons. This monoenergetic meson beam was passed through a 50 mil glass plate and 200μ C2 emulsion. Next to this plate three 200μ NTB stripped emulsions were added, all perpendicular to the meson beam. These emulsions were scanned and the mesons were grouped for each 65 micron depth of emulsion. The result is shown in Fig. 7.

As will be seen in the figure, the endings of the parallel beam of mesons spreads over 800μ depth. If the adjustment of thickness of absorbers is made correctly, then one can detect over 60 percent of the mesons with an emulsion thickness of 400 microns.

Comparison of the number of pions on each member of the pair of plates exposed for π^+/π^- experiments at the same time gives a criterion whether the adjustment of the thickness of the copper foil absorber in front of the glass plates was right or not. Then, based on the study of this projected range straggling curve, one can estimate the efficiency of pion detection with two layers of 200μ thick emulsion.

For the case of experiments of poor geometry, the conditions have not been well established as yet. In most cases the projected range straggling curves corresponding to slightly different energies are superposed and compensate each other, so that the resultant curve is almost flat.

The author should like to mention here that the broad spread of this projected range straggling curve indicates how complicated is the observation of single line spectrum such as the peak observed in the $p + p \rightarrow D + \pi^+$ reaction⁵ with the technique of a poor geometry. Not only the energy resolution but especially the computation of cross sections is expected to be fairly inaccurate.

6. Study of Prong Distribution of π^- Stars

This study has been already accomplished by several authors.⁶ The same statistics were also made on the results obtained here. The author should mention here that he admits that due to the lack of experience, especially in his early stage of scanning, he suffered some confusion in the definition of clubs.

Nevertheless, as shown in Fig. 8 the statistics were in good agreement with the results obtained by Adelman and Jones.⁶ The accuracy for the value of 69 percent for the probability of having one or more prongs on π^- stars is good enough for the present work.

ACKNOWLEDGMENTS

The author is grateful to Dr. W. Powell for the use of the magnet and to Dr. W. Barkas for his continuous interest and help throughout the work.

REFERENCES

1. R. Sagane and P. C. Giles, Phys. Rev. 81, 653 (1951); R. Sagane, Pasadena Meeting, Bull. Am. Phys. Soc. 27, No. 6, 17 (1952).
2. G. Miyamoto, Proc. Phys. Math. Soc. Japan 24, 676 (1942) and Proc. Phys. Math. Soc. Japan 17, 587 (1943); M. Sakai, J. Phys. Soc. Japan 5, 178 (1950); and R. Sagane and W. Gardner, UCRL Trans. III (1951).
3. C. Richman and H. A. Wilcox, Phys. Rev. 78, 496 (1950); M. Weissbluth, UCRL-568 (1950); W. Barkas and a group of Japanese physicists, private communication; M. M. Block, S. Passman, and W. W. Havens, Phys. Rev. 88, 1239 (1952); and H. W. Wilson and W. H. Barkas, Phys. Rev. 89, 758 (1953).
4. D. Clark, Phys. Rev. 81, 313 (1951); and D. Hamlin, M. Jakobson, J. Merritt, and A. Schulz, UCRL-1433 (1952).
5. W. F. Cartwright, C. Richman, M. N. Whitehead, and H. A. Wilcox, Phys. Rev. 78, 823 (1950) and 81, 652 (1951); W. F. Cartwright, Thesis, UCRL-1278 (1951); and V. Peterson, UCRL-713 (1950).
6. F. Adelman and L. Jones, Science, 111, 226 (1950); W. Cheston and L. Goldfarb, Phys. Rev. 78, 683 (1950); Menon, Muirhead and Rochat, Phil. Mag. 41, 583 (1950); and F. L. Adelman, Phys. Rev. 85, 249 (1952).

TABLES

- Table I Summary of results and target dimensions used for Al, C, and Be.
- Table II Summary of results and target dimensions used for Pb, Ag, and Cu.
- Table III The list of the π^+/π^- ratios for six elements at three energies.

Magnet Setting	8 Mev	13 Mev	8 Mev + 10^{10} Cu
Mean Energy	13 Mev \pm 3	10 Mev \pm 3	41 Mev \pm 2
	Number of Mesons π^+/π^-	Number of Mesons π^+/π^-	Number of Mesons π^+/π^-
Al	π^+ 217 π^- 61 2.4 	8 MEV SETTING π^+ 126 π^- 116 43 1.0 23 2.7 	π^+ 403 π^- 91 10
C	π^+ 217 π^- 61 1.5 	π^+ 536 π^- 76 5 	π^+ 1091 π^- 72 43 10.1 33 10.3
Be	π^+ 141 π^- 77 1.3 	π^+ 496 π^- 69 4.8 	π^+ 815 π^- 92 47 7 31 5.4

MU-4511

Table I

Magnet Setting	8 Mev	13 Mev	8 Mev + 10 mm Cu
Meon Energy	13 Mev ± 3	18 Mev ± 3	41 Mev ± 2
	Number of Mesons π^+/π^-	Number of Mesons π^+/π^-	Number of Mesons π^+/π^-
Pb	π^+ 84 A) 0.4 π^- 134 B) 0.6	π^+ 28 L. 1 π^- 17	π^+ 88 A) 5.8 π^- 13 B) 3.0
	μm THICK	μm THICK	μm THICK
Ag	π^+ 75 A) 0.63 π^- 81 B) 0.10	π^+ 24 L. 2 π^- 15	π^+ 189 A) 6.0 π^- 25 B) 4.0
	μm THICK	μm THICK	μm THICK
Cu	π^+ 197 A) 1.7 π^- 72 B) 2.0	π^+ 86 A) 1.7 π^- 37 B) 1.9	π^+ 234 A) 8.0 π^- 22 B) 7.4
	μm THICK	μm THICK	μm THICK

MU-4510

Table II

σ^2/σ^2 ratios at 95%

Signal setting	0 Hz	13 Hz	0 Hz + 20 th Hz
Mean Energy	13 Hz ± 3	18 Hz ± 3	23 Hz ± 3
76	0.47 ± 0.1	1.2 ± 0.6 ²	4.8 ± 2.5
82	0.70 ± 0.25	1.25 ± 0.7 ²	4.8 ± 1.5
86	2.0 ± 0.4	1.75 ± 0.5	6.7 ± 2.5
82	2.7 ± 0.8 ²	4.7 ± 0.8	10.5 ± 3.0 ²
0	1.95 ± 0.7 ²	5.7 ± 0.8 ²	11.0 ± 1.5
86	1.45 ± 0.7 ²	5.1 ± 0.9 ²	6.4 ± 1.0

20 Single run measurements

Detection efficiency for σ^2 below equal to 95%, for σ^2 as 95

Probability for having more than one ping store (including alias) is equal to 95

88J-4509

Table III

FIGURE CAPTIONS

- Fig. 1 Schematic diagram showing the experimental arrangement.
- Fig. 2 Plot of the π^+ production cross sections against atomic number of the targets.
- Fig. 3 Plot of the intensity distribution of the magnetic field against radius from the axis at 2-5/8 inch gap with magnetic field shapers in position.
- Fig. 4 Plot of the intensity distribution of the magnetic field against radius from the axis at 1-1/8 inch gap with simple cylindrical pole pieces only.
- Fig. 5 Plot of the number of π^+ endings against x-coordinate on the plate. The same was replotted against radius from the beam axis.
- Fig. 6 Plot of the number of π^+ endings against z-coordinate along the axis of the magnetic field. The sectional views of the pole pieces are also shown to give some idea of sharpness of vertical focusing relative to the gap distance.
- Fig. 7 The projected range straggling curve for 8 Mev $\pm 0.3 \pi^+$ mesons in emulsion.
- Fig. 8 Comparison of the data obtained in this experiment and those published by Adelman and Jones on number of prong distributions of π^+ stars.

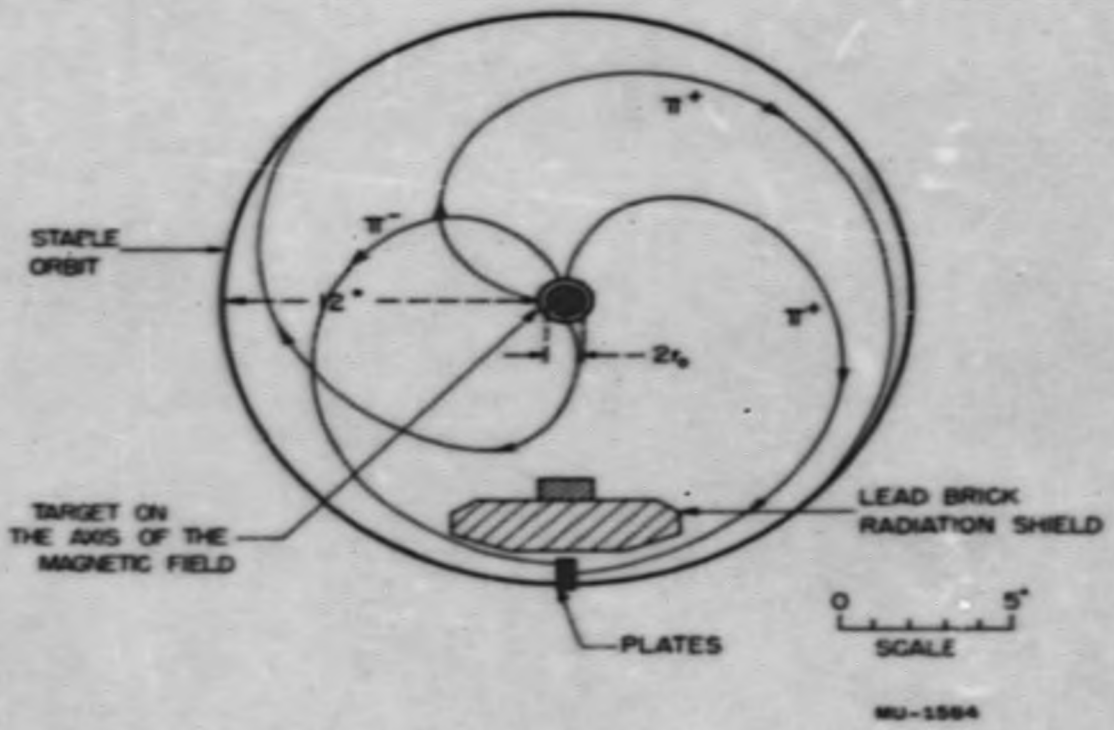


Fig. 1

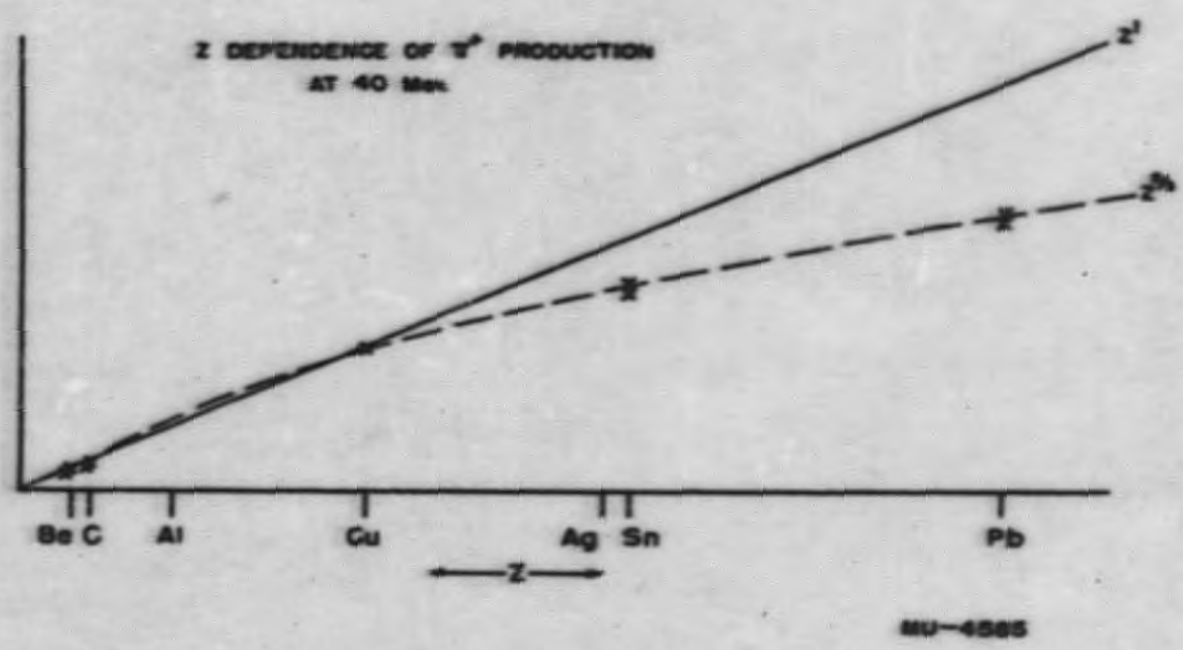


Fig. 2

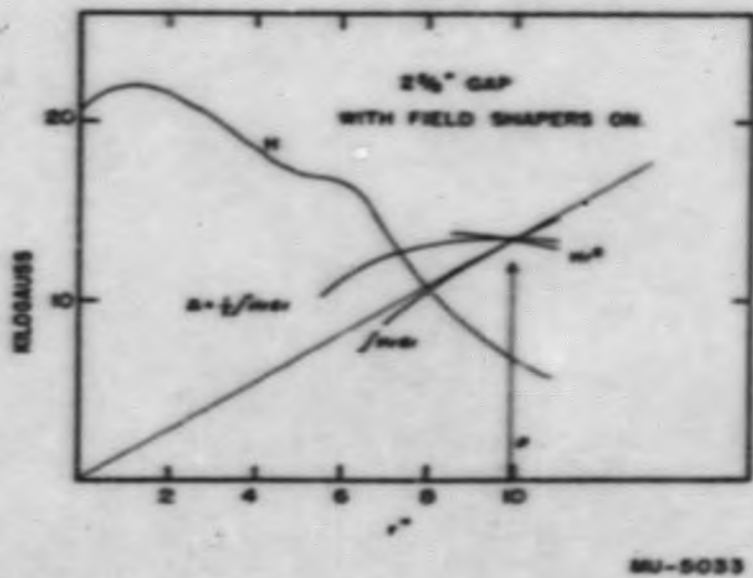


Fig. 3

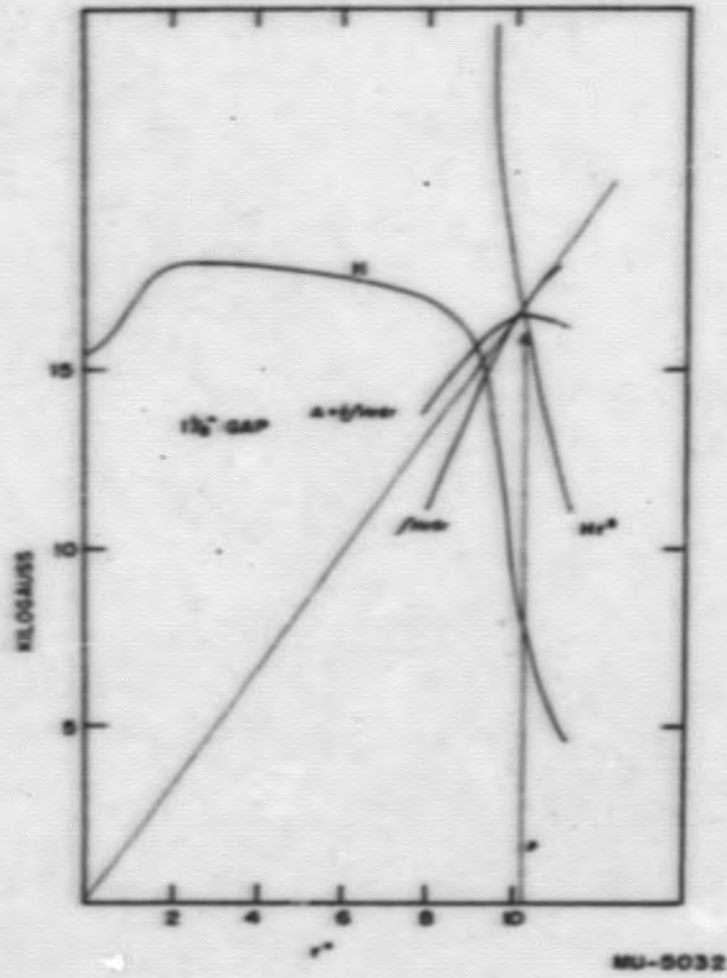


Fig. 4

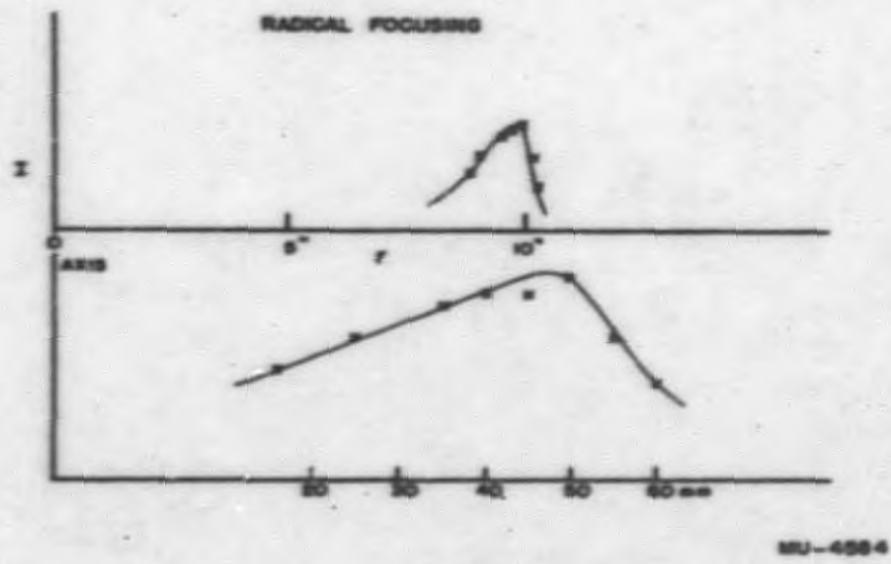
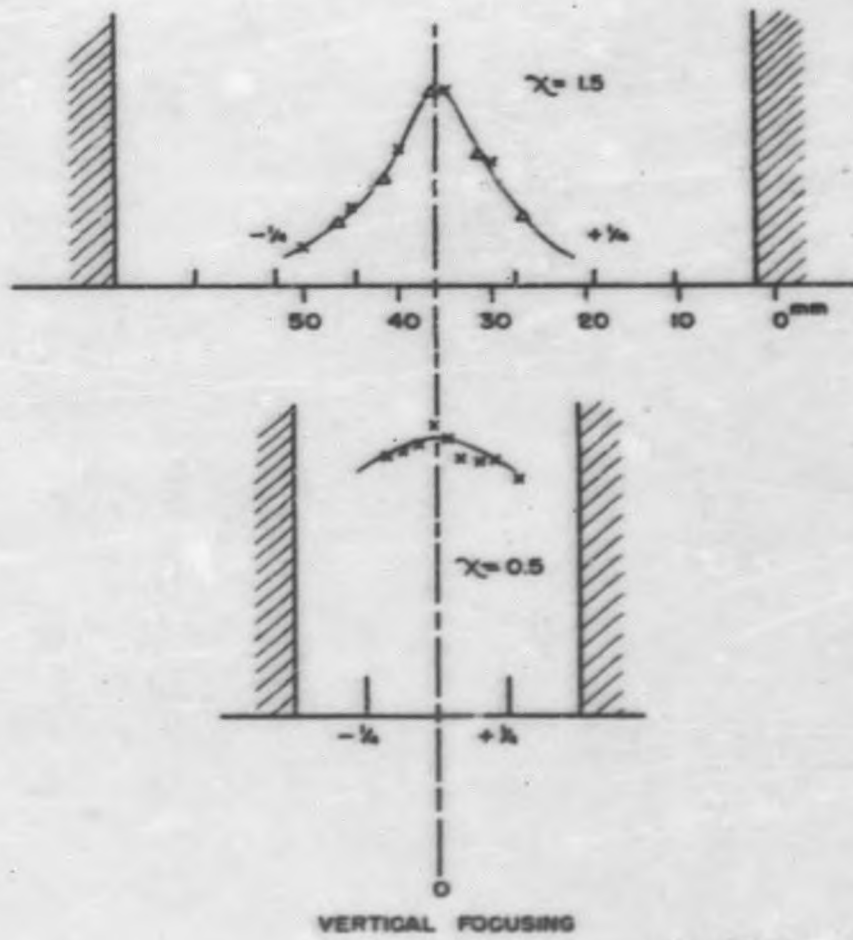
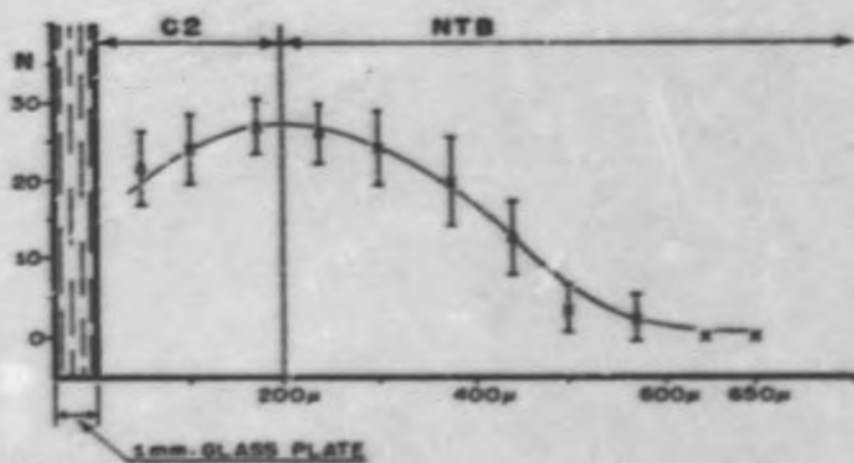


FIG. 5



MU-4586

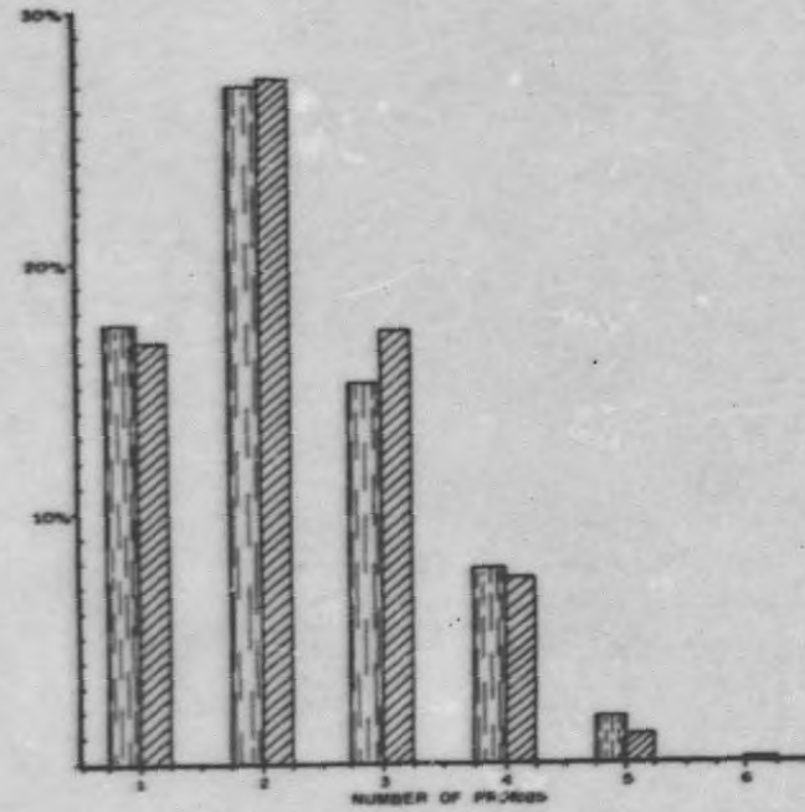
Fig. 6



PROJECTED RANGE STRAGGLING CURVE
FOR 8 MEV \pm 0.3 MEV π^+ MESONS.

MU-4513

Fig. 7



TOTAL 1004 K

MU-4512

Fig. 8

END